[7th] International Congress of Serbian Society of Mechanics
Sremski Karlovci, Serbia, June 24-26, 2019

# PRESSURE FIELD ANALYSES OF A LOW-RISE BUILDING MODEL SURROUNDED BY NEIGHBOURING BUILDINGS IN URBAN AREAS

**Kristina Kostadinović Vranešević[1], Anina Glumac[1], Ulf Winkelmann[2]**

[1] Faculty of Civil Engineering, University of Belgrade, Bulevar kralja Aleksandra 73, 11120 Belgrade, Serbia
e-mail: kkostadinovic@grf.bg.ac.rs, anina@grf.bg.ac.rs
[2] Ruhr-Universitat Bochum, Universitatsstr. 150, D-44801 Bochum, Germany
e-mail: Ulf.Winkelmann@rub.de

**Abstract**:

In this paper, pressure field over the roof of low-rise building model has been investigating using numerical simulations. The model is surrounded by four neighboring buildings of the same geometry as the principle one. The wind behavior around the building was simulated at wind angle of 45 degrees. Numerical calculations are performed using open-source code OpenFOAM. - Analysis solver for incompressible flow was applied using the Large Eddy Simulation (LES). The effect of different mesh types and inflow conditions are discussed. Two inlet definitions was implemented, one without prescribed turbulence, with the stream-wise velocity profile from the wind tunnel (WT), and another with the incoming flow turbulence synthetically generated using the divergence free synthetic eddy method (DFSEM). Numerical results of pressure distributions statistics are analyzed and systematically compared to the referenced experimental data. The results show that there is a significant influence of the inlet definition on the mean and standard deviation of pressure coefficient.

**Key words**: LES, low-rise building, turbulent inlet, surface pressure coefficient

## 1. Introduction

The loading effects of the natural wind on buildings are rather complicated interactive process between the wind flow and the various components of the building. The flow fields over the three-dimensional surface mounted building models are dominated by flow separation. This event has a great deal of importance in large number of applications such as wind load on structures, wind harvesting potential around the building, dispersion of pollutants, etc.
Many researchers have been attracted with issues of wind flow modelling around the buildings in urban areas which are characterized by low wind speed and high turbulence intensities compared to the rural areas. The experimental investigations in [1] and [2] and numerical in [3], [4], [5] deals with them. Dependence on the roof shape on the wind flow and turbulence intensities above the roof is demonstrated in [1]. The significant influence of the upstream building on the wind characteristics above the principal one is described in [2]. Numerical studies in [4] give the above

roof wind flow characteristics in three suburban landscapes characterized by houses with different roof profiles. Methods of synthetic turbulent inflow conditions are described in [4] and [5].
Aim of this paper is to model flow field for experimental case in [6] with a low-rise building model surrounded by four interfering buildings (case of group arrangement C2) with 45° wind angle. Large Eddy Simulations (LES) are performed leading to the numerical evaluation of unsteady pressure distributions for the building surfaces exposed to the wind action. The effect of different mesh types and inflow conditions are discussed. Two inflow definitions have been analysed, one with the streamwise velocity profile from WT tests exposed at the inlet and one synthetically generated turbulent inlet using a divergence-free modification of the synthetic eddy method (DFSEM) that has been proposed in [7].
Paper is organized into five sections. Section 2 refers to the experimental setup and describes the WT facility, model of the building and analysed configuration. Section 3 describes computational model adopted for the proposed simulations, geometry of the computational domain, together with the numerical schemes and the adopted turbulence model. In Section 4, the LES results are presented in terms of pressure statistics distributions, which are compared with WT measurements. The paper ends with conclusions in Section 5.

## 2. Wind tunnel setup

The insight in the experimental setup adopted to obtain data used in the following for the comparison with numerical results is presented in this section. Experiments were carried out in the atmospheric boundary layer WT of the Ruhr-University Bochum, Germany, within a Short Term Scientific Mission of the COST Action TU1304. WT has a rectangular cross-section, with weight, height and length of the test section 1.8m, 1.6m and 9.4m, respectively. Figure 1d presents the target configuration mounted in the WT. The approaching flow represents an urban wind exposure using the spire-roughness technique.

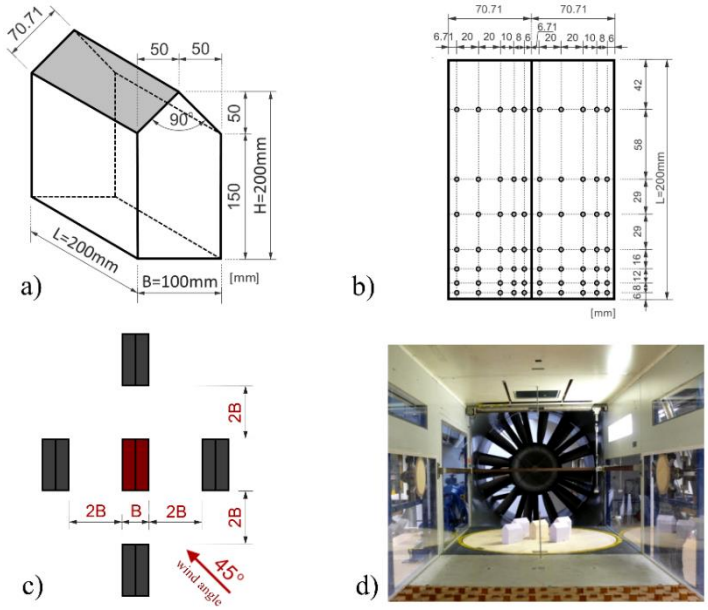


Figure 1. a) Geometry of the tilted house model, b) positions of the pressure measurement points on developed roof surface of the model, c) reference configuration, d) ref. configuration mounted in the WT

Tests were carried out on a 1:75$^{th}$ scale model of tilted house with roof inclination of 45°. The model dimensions, length (L), width (B) and height (H), are shown in Figure 1a. Reference configuration has principle building surrounded with the additional four interfering buildings,

Figure 1c,d and approaching wind angle of 45°. All buildings (principle and interfering ones) are of the same geometric characteristics. Surface pressure measurements have been carried out in 70 points on the roof of the principal building and their arrangement is given in Figure 1b. Sampling frequencies were 1000 Hz for pressure measurements. Results of experimental investigation are given in [6], which includes another configuration with only isolated principle building as well as three different approaching wind angles: 0°, 45° and 90° for both configurations.

## 3. Flow modelling

Three simulations have been run, using the OpenFoam©Finite Volume open source code to numerically evaluate the flow field for group arrangement with 45° wind angle experimental case in [6]. The geometry of the computational domain, together with the numerical schemes and boundary conditions are described in the following.

*LES modelling*

Unsteady flow around the group configuration is modelled using LES turbulence approach. Filtered incompressible, time-dependent Navier-Stokes equations are given by:

$$\frac{\partial \overline{u}_i}{\partial x_i}=0 \tag{1}$$

$$\frac{\partial \overline{u}_i}{\partial t}+\overline{u}_j\frac{\partial \overline{u}_i}{\partial x_j}=-\frac{1}{\rho}\frac{\partial \overline{p}}{\partial x_i}+\frac{\partial}{\partial x_j}\left(\nu\frac{\partial \overline{u}_i}{\partial x_j}\right)-\frac{\partial \tau_{ij}}{\partial x_j} \tag{2}$$

where $x$ and $t$ are the space and time coordinate, the overbar denotes the filtering operator (filter width is equal to grid size), $u$ and $p$ are the filtered velocity and pressure, $\rho$ and $\nu$ are the air density and kinematic viscosity, respectively and $\tau_{ij}$ the components of the subgrid-scale (SGS) stress tensor given by:

$$\tau_{ij}=\overline{u_i u_j}-\overline{u}_i\overline{u}_j \tag{3}$$

To close the system of equations (1) and (2) the Smagorinsky SGS model [8] is applied. The SGS stresses are determined via the SGS turbulent viscosity $\nu_{SGS}$ and the filtered rate of strain $\overline{S_{ij}}=\left(\partial u_i/\partial x_j+\partial u_j/\partial x_i\right)/2$:

$$\tau_{ij}-\frac{1}{3}\tau_{kk}\delta_{ij}=-2\nu_{SGS}\overline{S_{ij}} \tag{4}$$

Where $\nu_{SGS}=L_{SGS}^2\overline{S}$, in which $\overline{S}=\left(2\overline{S_{ij}S_{ij}}\right)^{1/2}$ is the characteristic filtered rate of strain and $L_{SGS}=\min(\kappa d, C_s V_c^{1/3})$ is the SGS mixing length, with $\kappa$ = 0.4187 the von Karman constant, $d$ the distance to the closest wall, $V_c$ the volume of the computational cell and $C_s$ = 0.135 the Smagorinsky coefficient. The near wall treatment is performed by adopting the wall function which provides a turbulent kinematic viscosity ($\nu_t$) condition for rough walls, based on velocity, using Spalding's law to give a continuous $\nu_t$ profile to the wall ($y+ = 0$).

The convection term in LES equations is discretized with Linear-upwind stabilized transport (LUST) scheme with a blending factor equal to 0.25. The LUST scheme is second order accurate and proved to be particularly successful for LES in complex geometries, offering a good trade-off between low dissipative behaviour and numerical stability [9]. The advancement in time is accomplished by the second order backward method. The pressure–velocity coupling is achieved by means of the pressure-implicit PISO algorithm.

*Computational domain and grid*

The computational domain dimensions together with the adopted reference system are reported in Figure 2a. The reference system origin is located in the middle of the inlet bottom line. The across-stream section is 9H wide and 8H high in accordance with the actual measures of the WT facility. Dimension in the wind direction is 24.5H. Ten rows of roughness elements with geometry and arrangement in agreement with the WT, are placed upstream the model. Their role is exposed in [3]. Distance of the building model to the roughness blocks is equal to 10H and to the outlet 10.5H. Geometry of the buildings under investigation is adopted like in WT, as it is shown in Figure 1a.

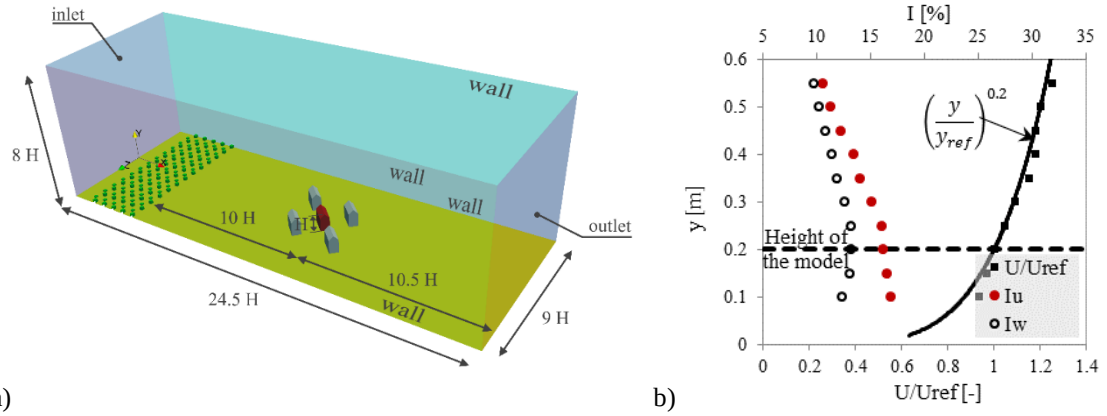


a) b)

Figure 2. a) Boundary conditions and computational domain, b) Mean stream-wise wind speed ($U/U_{ref}$) and turbulence intensities in stream-wise ($I_U$) and vertical ($I_W$) direction

The computational domain is discretized in two ways, first one is using blockMesh utility (Figure 3) and the second is using cfMesh (Figure 4), both implemented in OpenFOAM. For each grid, finer mesh is used near the building faces, the wake zone and the zone between the inflow and the building. In case of blockMesh high non-ortogonality occurs (max 75), due to the complex geometry of the domain. For cfMesh, distribution of the mesh size within computational domain is divided into four zones as illustrated in Figure 4. Similar zoning is adopted in [3] and [5].

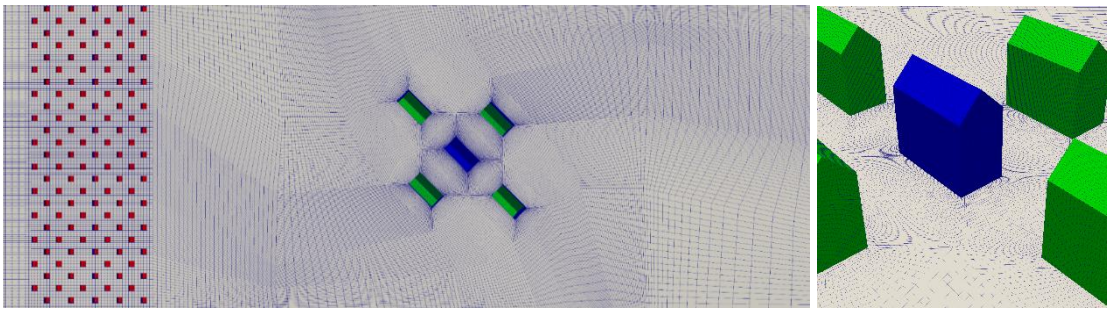

Figure 3. Mesh created using blockMesh utility

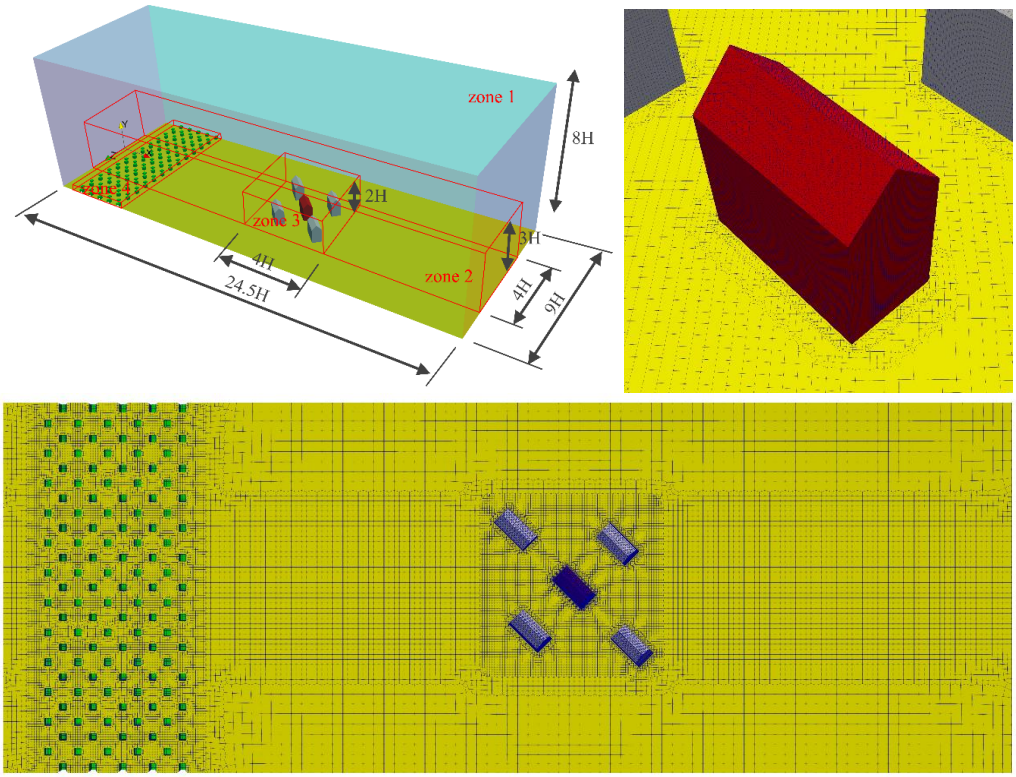


Figure 4. Mesh created using cfMesh: a) Dimensions of different mesh zones, b) mesh near the principle building, c) mesh near the bottom of the domain.

*Boundary condition*

The bottom of the domain as well as the lateral sides and the building surfaces and walls are modeled as a smooth wall, as it is in the WT. Two simulations have been run with different types of mesh (blockMesh and cfMesh) and same boundary conditions where at the inlet the stream-wise velocity profile obtained in WT tests at distance of 1m in front of the model, presented in Figure 2b, is exposed. Third simulation is run with cfMesh and synthetically generated turbulent DFSEM inlet defined in OpenFOAM, that has been proposed in [7]. Method generates inflow turbulence with prescribed mean velocity, turbulence length scales and Reynolds stresses, through a sum of synthetic eddies that are convected through a virtual box that encloses the inlet plane of the computational domain. These input parameters have been taken from WT measurements at the distance of 1m in front of the principal building at the height of the model. Mean stream-wise wind speed ($U_{ref}$) at the referent height (H=0.2m) is 13.8m/s and this value has been used to normalize the velocity profile given at Figure 2b. For the outlet a constant, zero static pressure is used.
Summary of characteristics of the performed numerical simulations is given in Table 1. Adopted time step for each simulation leads to a maximum Courant number in all simulations less than 1.

| **Case** | Mesh type | Mesh size [cells] | Inlet | Time step (max CoNum) | y+ values |
|---|---|---|---|---|---|
| **Case 1** | blockMesh | 2 802 700 | WT profile | $2.5 \times 10^{-5}$ (0.8) | mean: 25; max: 93 |
| **Case 2** | cfMesh | 573 554 | WT profile | $1 \times 10^{-5}$ (0.8) | mean: 33; max: 90 |
| **Case 3** | cfMesh | 573 554 | DFSEM | $1 \times 10^{-5}$ (0.9) | mean: 39; max: 105 |

Table 1. Characteristics of the performed numerical simulations

## 4. Results and discussion

In this section, the numerical results obtained for three cases defined in Table 1 are reported and compared to experimental data. Each simulation is run for a total time of 10s. In order to avoid flow initialization effects, the first 3.55s of simulations are discarded in the post-processing of the data, which corresponds to 10 flows through the domain (FTD). Generally, a minimum of 3-5 FTD are advised [10].

Contours of the mean surface pressure coefficients for all numerical cases (case1, 2 and 3) as well as for WT measurements are presented in Figure 5. Plots in Figure 6 shows comparison of experimental and numerical results of mean and standard deviation of pressure coefficient along four different lines on the roof of the principle building. The pressure coefficient, $C_p$ is calculated using the following expression:

$$C_p = (p - p_0) / (0.5 \rho U_{ref}^2) \tag{5}$$

Where with $p_0$, $\rho$ and $U_{ref}$ are denoted unobstructed stream pressure, air density and the reference velocity, respectively.

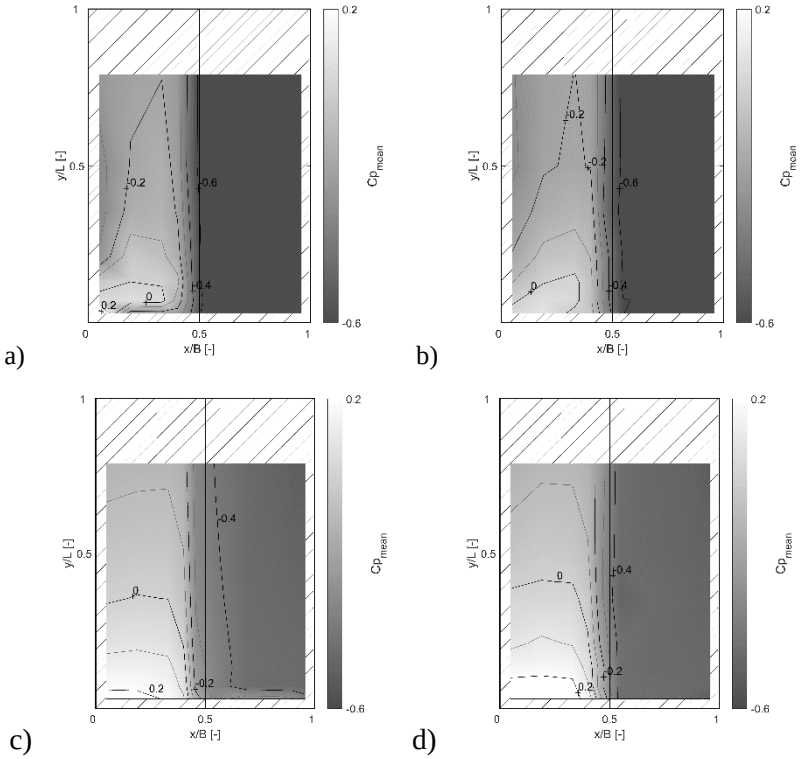


Figure 5. Contours of $C_{p,mean}$ coeficients on the roof of the principal low-rise building: a) $C_{p,mean}$ for WT measurements, b) $C_{p,mean}$ for Case 3, c) $C_{p,mean}$ for Case 1, d) $C_{p,mean}$ for Case 2

Numerical results of the mean pressure coefficient distribution in Figure 5c,d on the windward side of the roof shows overestimated values comparing to WT measurements. The reason may be found in inlet definition. In case 3 (Figure *5*. Contours of $C_{p,mean}$ coeficients on the roof of the principal low-rise building: a) $C_{p,mean}$ for WT measurements, b) $C_{p,mean}$ for Case 3, c) $C_{p,mean}$ for Case 1, d) $C_{p,mean}$ for Case 2Figure 5b) when turbulent DFSEM inlet is used results matches well the experimental, except in the zone close to the upstream edge. In this zone the small cone vortex exists in experimental results, but the same was not recorder in numerical simulations. The reason may be found in high y+ values on the surface of the model, for all cases they are higher

than 25. The suction on the leeward side of the roof in Case 0'1 and 2 is underestimated by LES. Good agreement has been achieved in Case 3. In Figure 5c,d a good agreement between results of numerical case 1 and 2 should be noticed, even though the mesh in Case 1 is finer and has five times more cells than the one adopted in Case 2. Also y+ values for both cases are close, as shown in Table 1.

When considering the standard deviation distribution of pressure coefficient over the roof numerical simulations in Case 1 and 2 failed to predict it, as it is shown in Figure 6. On the other hand, Case 3 gives a satisfactory results except in zone where the cone vortex has been occurred in experimental results, in which the values are underestimated. This shows the strong impact of inlet definition on $C_{p,RMS}$ coefficient.

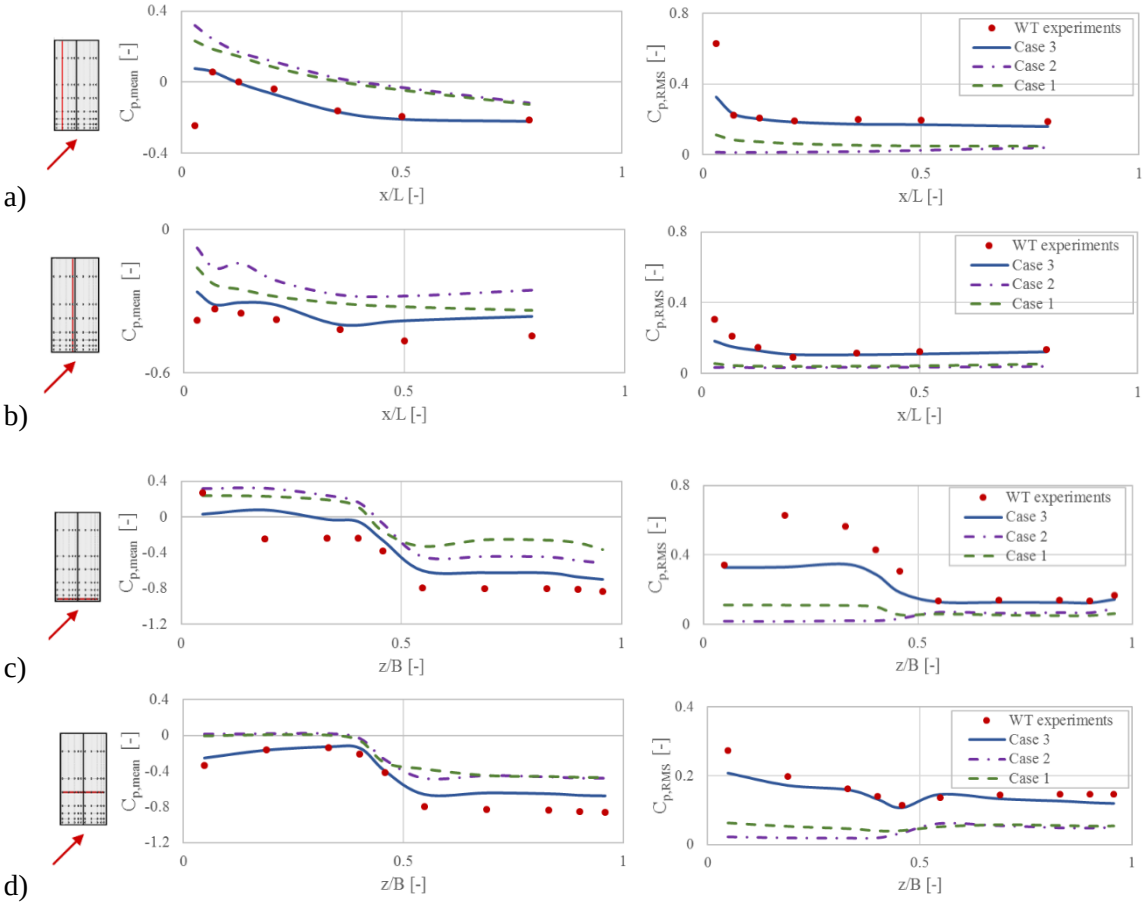


Figure 6. Comparison of mean and standard deviation distribution of pressure coefficient along four different lines on the roof of principle building: experimental and numerical resultes:
a) z/B=0.2, b) z/B=0.46, c) x/L=0.03, d) x/L=0.35

## 5. Conclusions

Summing up all the results, the importance of type and quality of the mesh may be noticed, as well as the inlet definition. According to different criteria, certain conclusions can be made for further analysis of flow field around buildings in urban areas:

- It is found that mean surface pressure coefficient on the roof predicted by LES when turbulent inlet is used are in good agreement with those obtained from experimental data, except in zones close to the upstream edges;

- Failure of Case 1 and 2 in prediction of mean surface pressure coefficient highlights the role of inlet definition in $C_{p,mean}$;
- Standard deviation of pressure coefficient is also strongly effected by inlet definition, where with turbulent DFSEM inlet a satisfactory results have been achieved;
- Regarding the type of the mesh, both types provides similar results, which leads to conclusion that further analyses should be carried out in the direction of type of mesh from Case 2 (cfMesh) due to the reduced computational costs comparing to mesh type in Case 1 (blockMesh), for such a complex geometries of the computational domain.

Future work will include simulations using finer mesh, with turbulent generators at the inlet. The analyses will be extended on the other wind flow characteristics.

## Acknowledgement

Numerical simulations were run on the PARADOX supercomputing facility at the Scientific Computing Laboratory of the Institute of Physics Belgrade, supported in part by the Ministry of Education, Science, and Technological Development of the Republic of Serbia under project No. ON171017. Also author KKV would like to acknowledge the financial support by the Ministry of Education, Science and Technological development of the Republic of Serbia, in the framework of the scientific project III 42012.

## References

[1] Rafailidis S., *Influence of building areal density and roof shape on the wind characteristics above a town*, Boundary-Layer Meteorol., vol. 85, 255–271, 1997.
[2] Šarkić Glumac A., Hemida H., and Höffer R., *Wind energy potential above a high-rise building influenced by neighboring buildings: An experimental investigation*, J. Wind Eng. Ind. Aerodyn., vol. 175, no. August 2017, 32–42, 2018.
[3] Ricci M., Patruno L., and de Miranda S., *Wind loads and structural response: Benchmarking LES on a low-rise building*, Eng. Struct., vol. 144, 26–42, 2017.
[4] Ledo L., Kosasih P. B., and Cooper P., *Roof mounting site analysis for micro-wind turbines*, Renew. Energy, vol. 36, no. 5, 1379–1391, 2011.
[5] Aboshosha H., Elshaer A., Bitsuamlak G. T., and El Damatty A., *Consistent inflow turbulence generator for LES evaluation of wind-induced responses for tall buildings*, J. Wind Eng. Ind. Aerodyn., vol. 142, 198–216, 2015.
[6] Kostadinović Vranešević K., Glumac A., and Hemida H., *Experimental investigation of wind flow around low-rise tilted house*, Zbornik radova 7. međunarodne konferencije Savremena dostignuća u građevinarstvu 2019, 2019.
[7] Poletto R., Craft T., and Revell A., *A new divergence free synthetic eddy method for the reproduction of inlet flow conditions for les*, Flow, Turbul. Combust., vol. 91, 519–539, 2013.
[8] Smagorinsky J., *General circulation experiments with the primitive equations. Part I: The basic experiment*, Mon. Weather Rev., vol. 91, no. 3, 99–164, 1963.
[9] Weller H., *Controlling the Computational Modes of the Arbitrarily Structured C Grid*, Mon. Weather Rev., vol. 140, 3220–3234, 2012.
[10] Thordal M. S., Bennetsen J. C., and Koss H. H. H., *Review for practical application of CFD for the determination of wind load on high-rise buildings*, J. Wind Eng. Ind. Aerodyn., vol. 186, no. December 2018, 155–168, 2019.